

Abdelfatah N. Aborobaa

Master student
Military technical college
Cairo
Egypt

Khaled A. Ghamry

Doctor
Military technical college
Cairo
Egypt

Amr Saleh

Doctor
Military technical college
Cairo
Egypt

Mohamed H. Mabrouk

Professor
Military technical college
Cairo
Egypt

Energy-saving and Performance-enhancing of a High Speed on/off Solenoid Valve

High-speed on/off solenoid valves (HSVs) are digital valves commonly used in hydraulic power systems. These valves are usually used in pressure and flow control which requires high dynamic and energy performance to improve the control accuracy. This paper aims to propose a new control method used to improve the dynamic and energy performance of HSVs. The proposed method is based on the pulse width modulation (PWM) technique implemented by LabVIEW software and NI myRIO. Based on that, NI myRIO has a real-time module; no feedback is needed. A mathematical model of the HSV is introduced, describing each subsystem of the valve and its interactions with each other. The proposed method is validated under different operating conditions. The results show that applying the proposed control method on the HSV will reduce the valve spool closing time by 72% and reduce energy consumption by 94% compared to the traditional on/off control method.

Keywords: High speed on/off valves, LabVIEW software, NI myRIO

1. INTRODUCTION

Control problems of fluid power systems can be solved using proportional or servo valves [1]. These valves provide good valve controllability and have the advantage of small hysteresis and high precision [2, 3]. However, these valves have defects such as high cost and high sensitivity to contamination [4, 5]. Digital valves have the potential to replace these valves as they have the advantage of high reliability and low cost. HSVs are typical digital valves commonly used in hydraulic and pneumatic power systems as they are low affected by pollution and have simple construction [6]. The HSV control system accuracy and response speed depend mainly on the characteristics of the HSV itself [7].

On the other hand, the successive reduction of the fuel resources, the continual raising in the fuel price, and the huge increase in environmental pollution make energy-saving an urgent issue for most researchers [8]. HSV is considered a basic component of hydraulic and pneumatic power systems. So, the energy efficiency of the whole system is significantly affected by the lost energy on the HSV [9]. Therefore, the dynamics and energy characteristics of HSV are considered its most important performance indicators.

Recently, many researchers have been interested in enhancing the dynamics and energy performance of HSV. Enhancing the dynamics and energy performance of HSV can be performed either by optimizing the driving algorithm or valve construction. A and Scheid et al. [10] used an electronic driving circuit to control the driving current instead of the excitation voltage to

improve the driving algorithm. Qi and Wang et al. [11] and Zhou et al. [12] used multi-voltage driving circuits to enhance the velocity response. While in Ref. [13], Tao and Ma applied conservation of energy at the HSV to study the relationship between the excitation voltage and the power loss. Zhong et al. [14] used the PWM technique with current feedback to improve the valve operating frequency and lower the solenoid coil temperature. In Refs. [15, 16], the robustness of a hydraulic actuator is enhanced by applying a self-correcting PWM control algorithm at HSV. Lee et al. [17] used high- and low-side current sensing circuits to develop a highly accurate solenoid valve driver.

Besides these studies and others, researchers also tried to improve the energy and dynamics characteristics by improving the valve construction. Liu et al. [18] used an annular flange and a permanent magnet to reduce the consumed energy by the HSV. Ruan et al. [19] designed a two-dimensional rotary valve used for the excitation of the hydraulic vibrator [20]. Xie et al. [21] designed a macro-micro linear actuator with high resolution and large stroke based on giant magnetostrictive material. Noergaard et al. [22] built a moving magnet actuated (MMA) annular seat valve to avoid the solenoid valve switching limitations. Koktavy et al. [23] developed a new valve architecture where two spools driven by crank-mechanism are used.

Improving the dynamics and energy performance of HSV through improving the valve construction is available only at the stage of valve design. Otherwise, this method cannot be used to enhance the performance of existing HSVs.

All of the above researches are concerned with improving the dynamics performance of HSVs. But, few of these researches are concerned with improving both the dynamics and energy performance of HSVs. Even if the energy performance is improved, a relatively small energy ratio is obtained. As well, few researchers

Received: November 2021, Accepted: February 2022

Correspondence to: Abdelfatah N. Aborobaa
Military technical college, Ismail Al Fangari, El-Qobba
Bridge, Cairo, Egypt.

E-mail: abdelfatah.nader@mtc.edu.eg

doi:10.5937/fme2201283A

© Faculty of Mechanical Engineering, Belgrade. All rights reserved

FME Transactions (2022) 50, 283-293 283

studied their proposed method under different operating conditions.

Therefore, the main contribution of this paper is to propose a control method that enhances both the dynamics and energy performance of HSVs with a large ratio of saved energy. Moreover, the proposed control strategy is studied under different valve operating conditions.

The proposed control method is implemented by NI myRIO, which is programmed using a LabVIEW state machine. NI myRIO is a reconfigurable input/output device used for real-time implementation of multiple design or control concepts [24]. This device can be programmed using LabVIEW or C. In this work, LabVIEW is used to program NI myRIO, as the software of the control system developed by LabVIEW has the advantage of visualized programming, fast development, and clear structure [25].

In this paper, valve construction and its principle of operation are explained in section 2. A mathematical model based on differential equations describing each subsystem of the valve is presented in section 3. An explanation of the proposed control method, containing the LabVIEW state machine code and the implemented hardware setup, is given in section 4. Experimental setup and the required parameters identification are presented in section 5. While in section 6, results are discussed. Finally, the conclusions are presented in section 7.

2. HSV STRUCTURE

The HSV under this study is (HSV-6432-B). It has three positions and four ways. Figure 1 shows a typical 4/3 solenoid operated direction control valve [26].

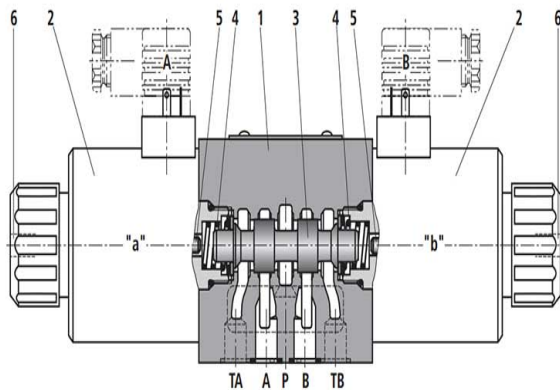


Figure 1. A typical HSV; two solenoids "a" and "b," (1) valve body, (2) solenoid coil, (3) valve spool, (4) return spring, (5) solenoid plunger, (6) press pin.

As shown, the valve has two solenoids on each side. When either of these solenoids is energized, an electromagnetic force is produced. This force pushes the solenoid plunger, which moves the valve spool against the return spring force.

The four ports of the valve are the supply port (P) connected to the pump, the return port (T) connected to the tank, and two ports (A) and (B) connected to the hydraulic actuator.

The three positions of the valve spool are neutral, "a," and "b" positions. The neutral position is obtained

when neither of the two solenoids is energized. Therefore, the valve spool is kept stationary at the neutral position under the action of the two springs. Position "a" is obtained when solenoid "a" is energized. Position "b" is likely obtained when solenoid "b" is energized. The press pin at the end of each solenoid is used for manual valve operation. When the spool is neutral, hydraulic oil is prevented from passing to the actuator. Positions "a" and "b" allow the hydraulic oil to flow to the actuator. If the valve spool is at position "a," the supply port is connected to port (A), allowing the hydraulic oil to pass to the actuator through that port, while port (B) is connected to the tank. If the valve spool is at position "b," hydraulic oil is allowed to pass to the actuator through port (B) while port (A) is connected to the tank.

3. HSV MATHEMATICAL MODEL

In this section, a mathematical model for HSV is presented. As shown, the HSV can be represented by two main subsystems; the electromagnetic subsystem and the mechanical subsystem. Figure 2 shows the HSV main subsystems and their interactions.

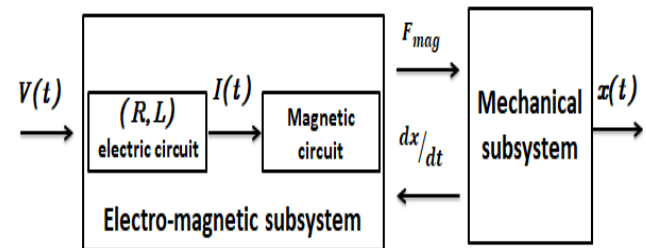


Figure 2. Representation of HSV subsystems and their interactions.

3.1 Electromagnetic subsystem

Figure 2 also shows that the electromagnetic can be represented by an (R, L) circuit. Consequently, the total solenoid applied voltage can be expressed as follows:

$$U_t = iR + i \frac{dl}{dt} + L \frac{di}{dt} \quad (1)$$

where U_t ... is the solenoid driving voltage [V].

i ... is the solenoid coil passing current [A].

R ... is the solenoid coil resistance [Ω].

L ... is the solenoid coil inductance [H].

The solenoid coil inductance is a function of the valve spool position, and it can be expressed as shown in equation (2), while its derivative with time is expressed in equation (3).

$$L = \frac{\mu_o An^2}{(g_{\max} - x)} \quad (2)$$

$$\frac{dL}{dt} = \frac{\mu_o An^2}{(g_{\max} - x)^2} \frac{dx}{dt} \quad (3)$$

where μ_o ... is the air gap permeability [H/m].

n ... is the number of solenoid coil turns.

g_{\max} is the maximum length of the air gap [m].

x is the valve spool position [m].

A is the air gap cross-section area [m²].

From equations (2) and (3), the time derivative of the coil inductance can be expressed as follows:

$$\frac{dL}{dt} = \frac{L}{(g_{\max} - x)} \frac{dx}{dt} \quad (4)$$

Hence, the current derivative can be expressed as:

$$\frac{di}{dt} = \frac{1}{L}(U_t - iR) - \frac{i}{(g_{\max} - x)} \frac{dx}{dt} \quad (5)$$

3.2 Mechanical subsystem

The following equations can represent the mechanical subsystem of the solenoid valve

$$F_{mag} - F_{hyd} - K(x + x_{pre}) - c\dot{x} = m\ddot{x} \quad (6)$$

where F_{mag} is the electromagnetic force [N].

F_{hyd} is the hydraulic force [N].

K is the return spring stiffness [N/m].

x_{pre} is the pre-loaded spring distance [m].

c is the damping coefficient [N.s/m].

m is the mass of the moving parts [kg].

Equation (6) shows that the electromagnetic force is the spool movement motivation force. The spool movement restriction forces are the hydraulic force, spring force (Kx), and damping force ($c\dot{x}$).

The electromagnetic force can be expressed as [27]:

$$F_{mag} = \frac{1}{2} \frac{\mu_0 n^2 A i^2}{(g_{\max} - x)^2} \quad (7)$$

Rabie, M Galal et al. [28] derived an expression for the hydraulic force. It can be expressed as :

$$F_{hyd} = 0.248\omega\Delta P x \quad (8)$$

where ω is width of the solenoid valve port [m].

ΔP is the pressure difference between both sides of the valve spool [Pa].

When the valve is excited, the electromagnetic subsystem of the valve is responsible for converting the excitation voltage into force. This force is responsible for overcoming the valve spool restriction forces and makes the spool move to the fully open position.

When the valve spool reaches its maximum stroke, it stops, and equation (6) becomes:

$$F_{mag} - F_{hyd} - K(x + x_{pre}) = 0 \quad (9)$$

Now, the electromagnetic force is only required to hold the valve spool at its position overcoming the hydraulic and spring forces.

As explained in equation (7), the electromagnetic force is directly proportional to the solenoid current. So, the needed force is large at the beginning of solenoid

energizing. Consequently, a large electric current should be consumed to quickly overcome the restriction forces and reduce the valve opening time. If the spool reaches its maximum stroke, a small force is required, and hence small current should be consumed.

From equations (9&7), the values of the required holding force and the corresponding holding current could be obtained. The excess consumed electric current is converted to heat, raising the temperature of the solenoid. The solenoid temperature rise is a function of the solenoid architecture and the excessive consumed current. So the solenoid current can be divided into two main parts:

$$i_{tot} = i_{hol} + i_{temp} \quad (10)$$

where i_{hol} is the holding current, and i_{temp} is the excess current converted to heat.

Generally, the electric power and energy are expressed as ($P = i^2 R$) and ($W = Pt$) respectively. So, the power and energy lost due to consuming excess current can be expressed as :

$$P_{los} = i_{temp}^2 R \quad (11)$$

$$W_{los} = P_{los} t \quad (12)$$

where P_{los} is the power lost [W].

W_{los} is the energy lost [J].

t the valve operating time [s].

4. PRINCIPLE OF THE PROPOSED CONTROL METHOD

In this section, the principle of the proposed control method is presented. This method uses state machine language and NI myRIO as a controller. This method does not use any sensor to give feedback.

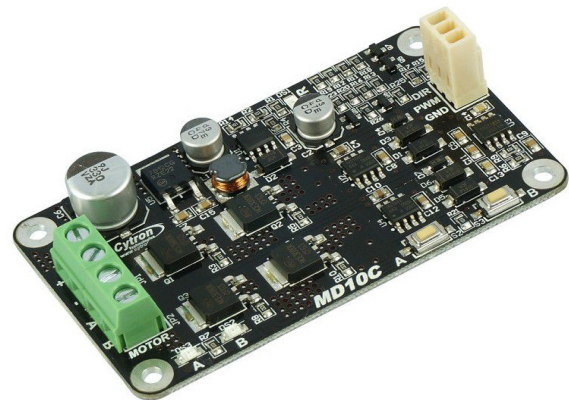


Figure 3. MD10C driver card.

MD10C driver card, shown in figure 3, is used to drive the excitation voltage to the solenoid valve according to the control signal from the controller.

As shown in the figure, the card has four ports on the left side; two for the power supply (+, and -) and the others (A and B) are connected to the solenoid valve, while on the right side, there are three ports; port (GND) is connected to ground, and the two others (PWM, and DIR) are the control signal ports.

The excitation signal from the power supply to the valve is delivered correspondingly to the control signal at the PWM port. The control signal at the DIR port controls the excitation signal direction. If there is no signal at the DIR port, the signal is delivered from port A to port B and vice-versa.

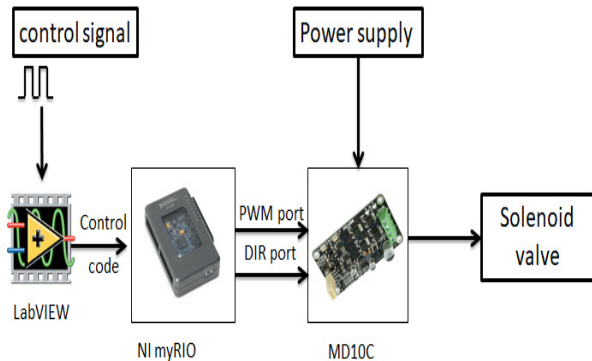


Figure 4. Hardware implementation of the proposed control method.

The hardware implementation of the proposed control technique is shown in figure 4, in which a 24 DC voltage source is used as a power supply connected to the driver card. LabVIEW software defines the operating code to NI myRIO accordingly to the desired control signal.

The controller then feeds the control ports of the driver card according to the proposed control code. Finally, the driver excites the valve with the controlled excitation voltage.

The control strategy is written using state machine language and implemented using LabVIEW software. Figure 5 shows the principle of the control method. The desired input control signal is generated with time by the operator. The control code should define two variables (t_{on} & t_{off}) whose values depend on the operator input signal. The variable t_{on} 's value is when the operator controls the input signal starts rising. While the value of the variable t_{off} is the time at which the control input signal starts dropping down. The values of variables (t_0 , t_c and d_{ch}) should be accurately determined. t_0 is a time more extensive than that the spool takes to make the valve fully open. t_c takes less time than the spool to start moving back to its initial position. d_{ch} The control signal duty cycle is adequate to feed the solenoid valve with the holding electric current i_{hol} . The method of determining these values is explained in the next section.

Once the operator input signal starts, the controller transmits a PWM signal with a duty cycle with a value equal to one to the PWM driver port. That helps rapid open the valve spool.

After a time equal to t_0 , the valve spool should have been moved to its maximum stroke. Then, the PWM signal duty cycle is reduced to d_{ch} as only the holding current is adequate, any more current is not needed, and considered a waste of power. The controller does not transmit any signal to the driver's DIR port at these two conditions.

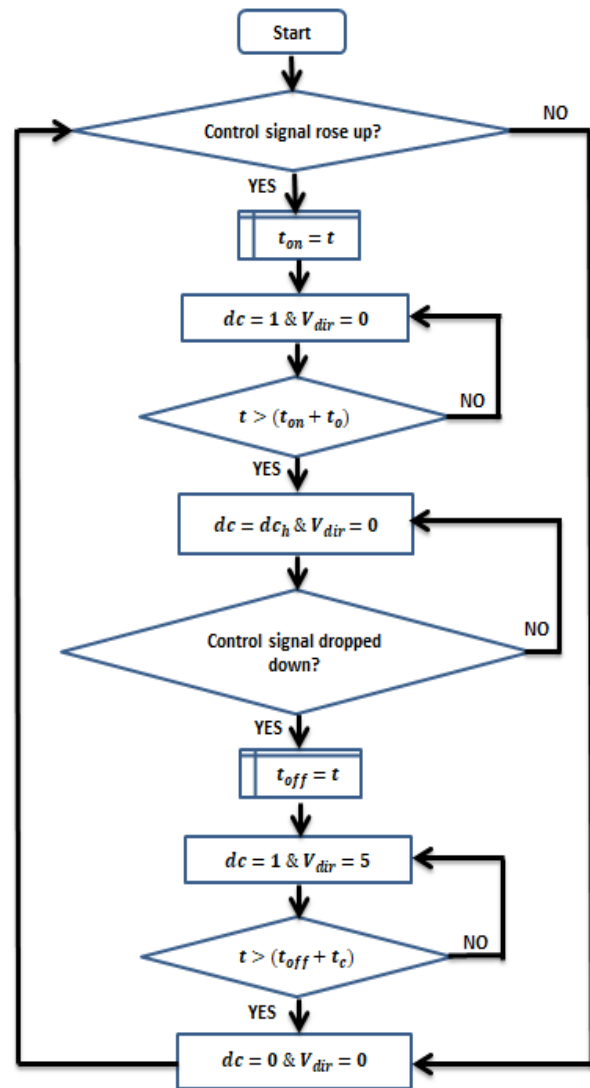


Figure 5. Control method flow chart.

If the operator input signal starts dropping down, the solenoid valve is to be de-energized. According to Lenz's Law, when the solenoid is de-energized, an induced emf is produced opposing the motion of the valve spool. Consequently, the controller transmits two signals; one of five volts to the driver DIR port, and the other is a PWM signal with a duty cycle having a value of one to the driver PWM port.

That will feed the solenoid valve with a complete negative supply voltage. This voltage will face the induced emf and hence reduce the time taken by the spool to close the solenoid valve. After a time equal to t_c , the solenoid valve is de-energized. The driver prevents any voltage from transmitting to the valve as no signals are received from the controller.

5. EXPERIMENTAL SETUP AND PARAMETER CALCULATIONS

Equation (5), in section 3, shows that the time derivative of the solenoid coil current depends on two parts. The first part is affected by the solenoid electromagnetic properties, while the second part is affected by the valve spool dynamics.

The equation shows that any change in the valve spool position will change the time derivative of the coil passing current. Any change in valve spool position would change the current curve. Hence, the slope of the current curve can be used to estimate the valve spool movement. If the valve spool is fixed stationary, when the solenoid is energized, the second part of the equation will be zero. Consequently, the current will increase exponentially until reaching its maximum value. Similarly, if the spool is fixed stationary when the solenoid is de-energized, the current will drop exponentially until reaching its neutral position.

Solenoid current is measured when the solenoid valve is energized and de-energized while its spool is fixed stationary at a certain point and prevented from motion. The electric current is measured when the solenoid spool is fixed at two positions, its initial position and its maximum stroke position. Fixation of the spool at either point is carried out using a mechanical jaw.

A resistor is connected with the solenoid to measure the electric current passing through its coil. As the resistor is connected in series, the passing current through the solenoid and the resistor is the same.

The resistor is ceramic-based, having a maximum power of 20 W. Consequently, it can withstand the high consumed current. The resistor is 1 ohm. So, its voltage drop equals its passing current. A NI USB-6008 data acquisition card measures the voltage drop across the resistor, which is equal to the solenoid passing current.

The solenoid current measured is shown in figure 6. The figure shows that the current curve slope does not change until it reaches its maximum value when the solenoid is energized. Also, when the solenoid is de-energized, the current curve slope does not change until the current reaches zero. The figure declares a difference between the current curve slopes when the spool is fixed at its neutral position and its maximum stroke. That is because of the difference in the inductance at the two positions. The figure also shows that the maximum value of the current when the spool is fixed at its initial position is higher than when the spool is fixed at its maximum stroke. The force required for maintaining the spool at its initial position is larger than that required for maintaining the spool at its maximum stroke.

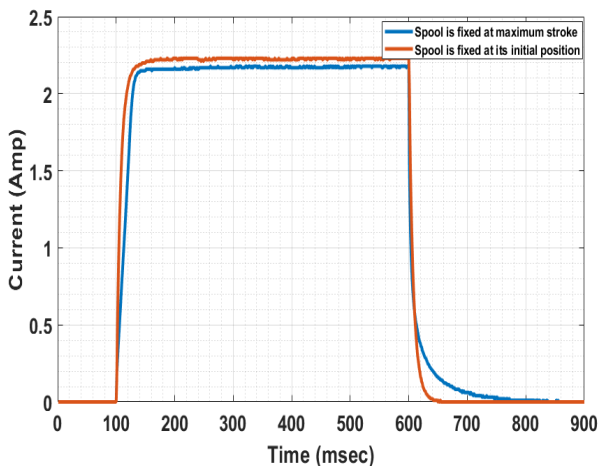


Figure 6. The current is measured when the valve spool is fixed at its initial position and when it is fixed at its maximum stroke position.

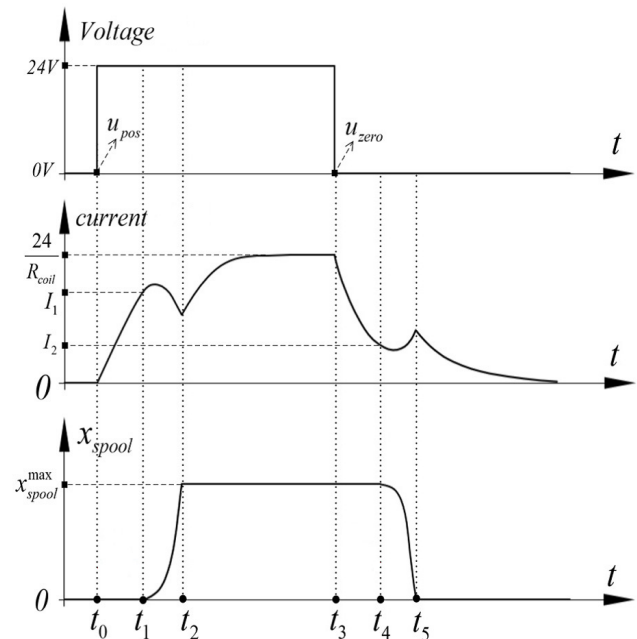


Figure 7. A typical response of a solenoid valve shows the excitation voltage, current, and displacement.

Figure 7 shows a typical response of a solenoid valve [29]. The figure shows the energizing voltage, the corresponding current, and spool displacement.

As shown, after the valve has been energized, the current curve may be used to measure the time taken by the spool to start moving and the time taken to reach maximum stroke.

The current curve also can be used to determine the time taken by the spool to start moving back and to reach zero position after it has been de-energized.

The solenoid current is measured when the solenoid is excited by a pulse excitation signal, having an amplitude of 24 volts and a frequency of 2 Hz. These transition times are calculated for the solenoid valve under this study. The result of the measured current is shown in figure 8.

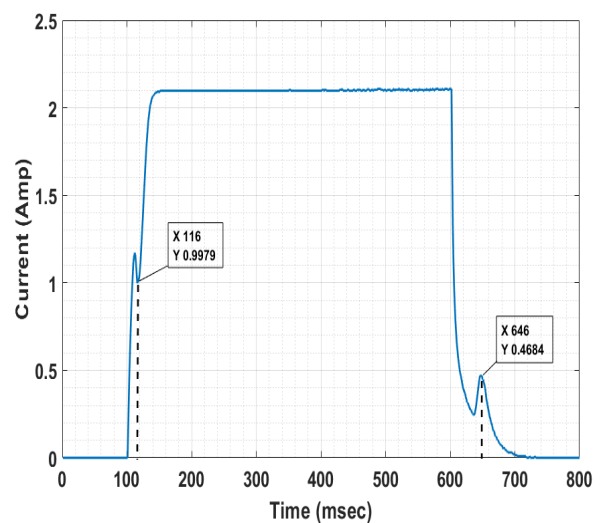


Figure 8. Solenoid valve passing current after it has excited by a pulse signal of amplitude 24 volt and frequency 2 Hz.

The figure shows that the spool takes about 16 msec, after the solenoid has been energized, to reach its maximum stroke. The value t_0 is chosen to be 25 msec.

This value will ensure that the valve has been fully opened under different operating conditions.

It is also shown; that the spool takes about 46 msec to move back to its initial position after the solenoid has been de-energized. So the value t_c is chosen to be 8 msec. This value is adequate to shorten the time taken by the spool to move back to its initial position.

Spring and hydraulic forces should be calculated to estimate the holding duty cycle value. Figure 9 shows an experimental test set up to measure the spring stiffness. The spring is subjected to various forces by changing the loading masses. At each load, the spring deflection is measured. Then, a linear relationship between the spring deflection and the corresponding load is obtained to estimate the spring stiffness.

The electromagnetic force required to hold the valve spool at its maximum stroke can be obtained by substituting (9) with the parameters shown in table 1.

Table 1. Spring and hydraulic forces parameters identification

Parameter	Unit	Value
Spring stiffness(K)	N/m	5600
Valve spool maximum.stroke (x)	m	$1.7 * 10^{-3}$
Pre-loaded spring distance (x_{pre})	m	$1.5 * 10^{-3}$
Valve port width (ω).	m	$25 * 10^{-3}$

Also, the actual generated force after the solenoid valve is energized is measured. That can be done by energizing the solenoid valve and letting the spool reach its maximum stroke. Then the valve spool is subjected to an axial load created by standard weighted masses. Masses are added until the valve spool is to move back. Hence, the generated electromagnetic force equals the exerted axial load.



Figure 9. Experimental setup to measure the spring stiffness.

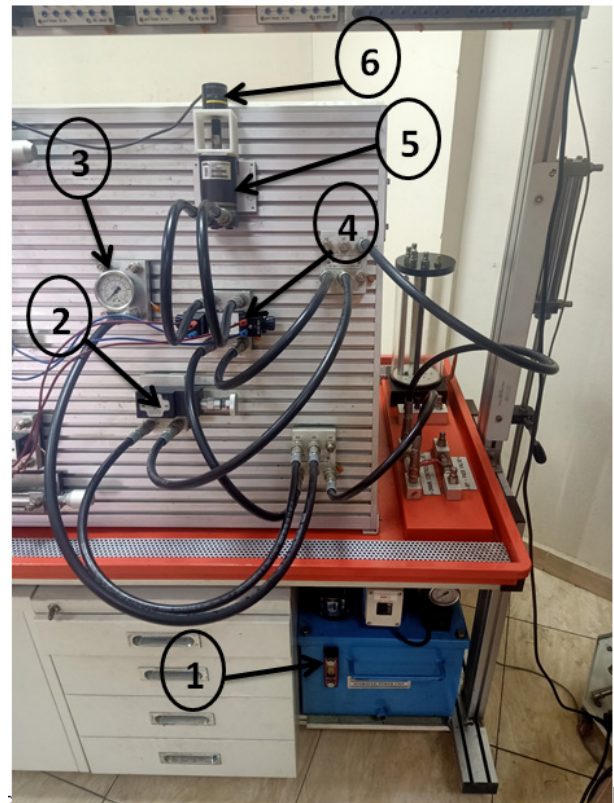


Figure 10. A hydraulic circuit is set up to measure the hydraulic motor speed. (1) hydraulic tank. (2) relief valve. (3) pressure gauge. (4) solenoid valve. (5) hydraulic motor. (6) rotary encoder.

Equation (7) shows that the electromagnetic force is directly proportional to the electric current square for the same spool position. Consequently, the required holding current and the corresponding holding duty cycle can be obtained by comparing the required force with the solenoid valve generated force and consumed electric current. The experimental results show that the needed duty cycle is 0.2. However, a duty cycle of 0.22 ensures holding the spool at different operating conditions.

The hydraulic circuit shown in figure 10 is installed to validate the proposed control method. This circuit consists of the solenoid valve under this study which is connected to a hydraulic motor. A rotary encoder is installed on the hydraulic motor to measure its speed. The base that attaches the encoder with the hydraulic motor is produced using a 3D printer.

The used rotary encoder is (E6B2-CWZ6C), which produces 1000 pulse/rev [30]. The encoder is connected to NI myRIO, and a LabVIEW code depending on the shift register, is designed to measure the motor speed.

The solenoid valve is energized either by the traditional or proposed control methods. Also, the valve supply pressure is changed. At every time, the hydraulic motor speed is measured.

A comparison between these speeds is made to validate the proposed control method.

6. RESULTS AND ANALYSIS

The solenoid supply voltage can be reduced by using the PWM technique. Using the PWM technique directly without applying the proposed control method will

reduce the consumed energy, but other unsolicited results will appear. The solenoid valve is excited for 0.5 sec by a PWM signal with a frequency of 1 kHz and different duty cycles. The current is measured, and the results are shown in figure 11. The figure shows that, when applying a signal with a 30% duty cycle, the current increases exponentially until reaching its maximum value without any change in its slope. Also, the current decreases exponentially to zero without changing its slope. So, the valve spool does not move from its position. Consequently, applying a PWM signal with a 30% duty cycle or lower will produce an electromagnetic force not adequate to overcome the static friction force and other motion restriction forces.

When applying a PWM signal with a 40% duty cycle or higher, the current will oscillate until reaching its maximum value. As explained in the previous section, any change in the existing electric slope is due to the valve spool movement. So, the oscillation of the current curve indicates that the spool oscillates until it settles at its maximum stroke. Consequently, the last oscillating point before the electric current increases exponentially to its maximum value indicates the point at which the valve spool has been settled at its

maximum stroke position. The zooming view (zoom 1) shows that point for different duty cycles. The zooming figures are concerned with indicating the time at which the valve spool has been settled. So, the electric current curve resulting from using a PWM signal with a 30% duty cycle is removed.

The valve spool takes to settle at its maximum stroke position about 140, 61, and 42 msec when energized by a duty cycle of 40%, 50%, and 60%, respectively.

Decreasing the applied duty cycle will reduce the time taken by the valve spool to return to its initial position. The zooming view (zoom 2) shows the points at which the valve spool has been moved back to its initial point. It is shown that when the solenoid valve is de-energized, the valve spool takes to move back to its initial position 40, 42, and 45 msec when applying a duty cycle of 40%, 50%, and 60%, respectively.

Therefore, reducing the applied voltage by applying the PWM technique directly without using the proposed control method will decrease relatively the consumed energy. But the valve spool will oscillate and take a long time to settle at its maximum stroke when the valve is energized.

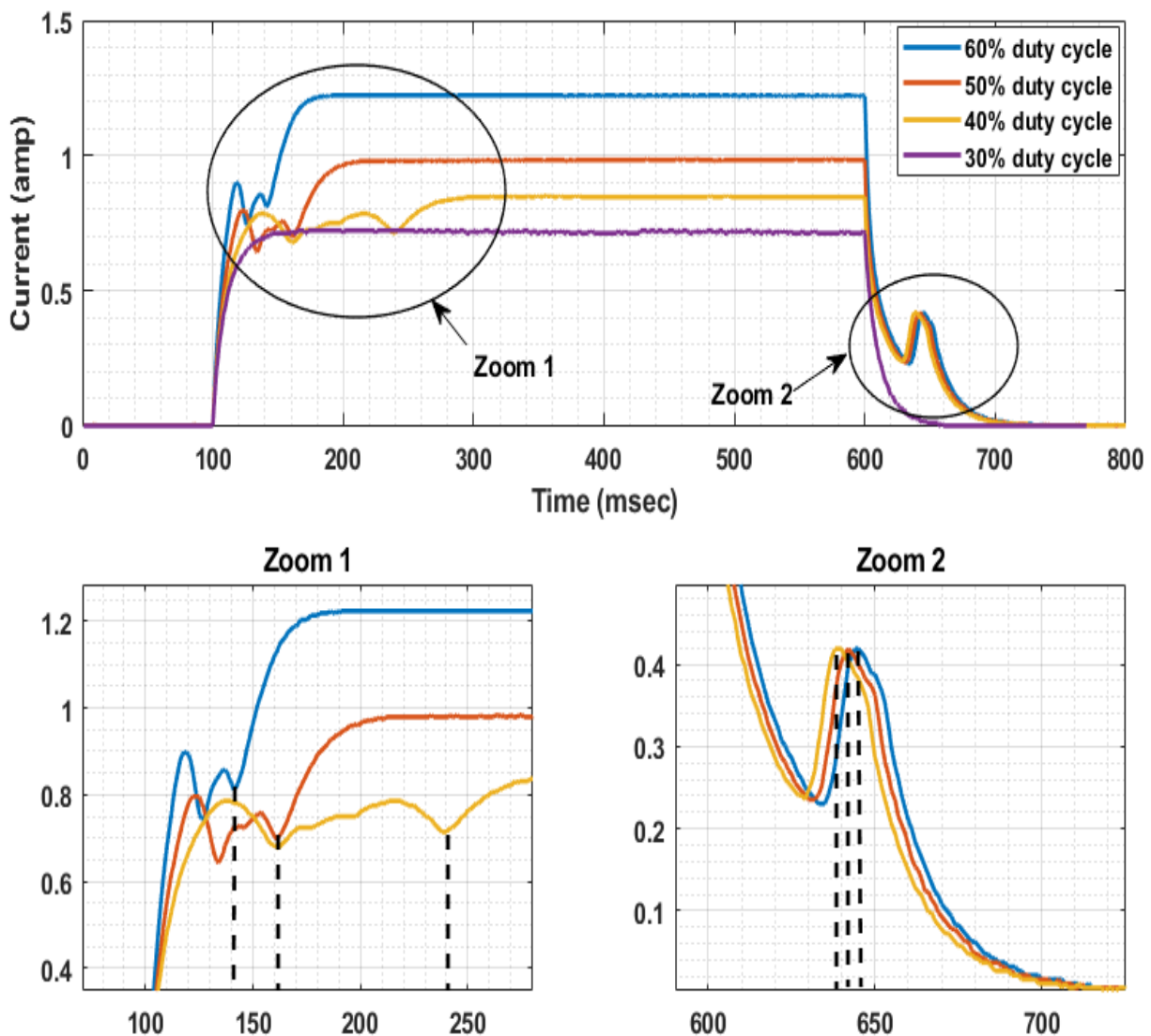


Figure 11. Solenoid current when the solenoid is excited for 0.5 sec by a signal of frequency 1 kHz and different duty cycles (60%, 50%, 40%, and 30%).

The time taken by the valve spool to return to its initial position when the solenoid is de-energized will decrease. However, the resulting reduced time is short.

The proposed control method is applied to the solenoid valve using state flow and the parameters identified in section 5. The delivered signal from NI myRIO to the driver card control ports is shown in figure 12.

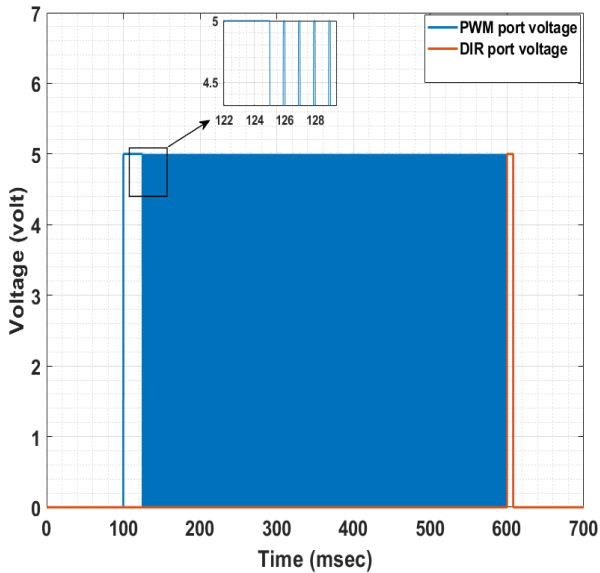


Figure 112. The driver card control ports voltage according to the proposed control code.

The corresponding average voltage delivered from the card to the solenoid valve is shown in figure 13. Also, the figure shows a comparison between the solenoid valve average delivered voltage when using the proposed control method and the solenoid valve delivered voltage when using the traditional on/off control method.

The solenoid valve is energized by using both traditional and proposed control methods. The passing current is measured, and the results are shown in figure 14.

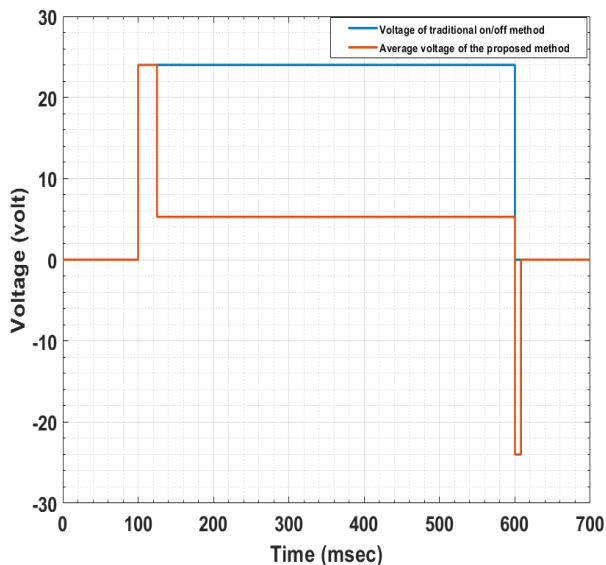


Figure 123. The solenoid delivered voltage using the traditional on/off method, and the average delivered voltage when using the proposed control method.

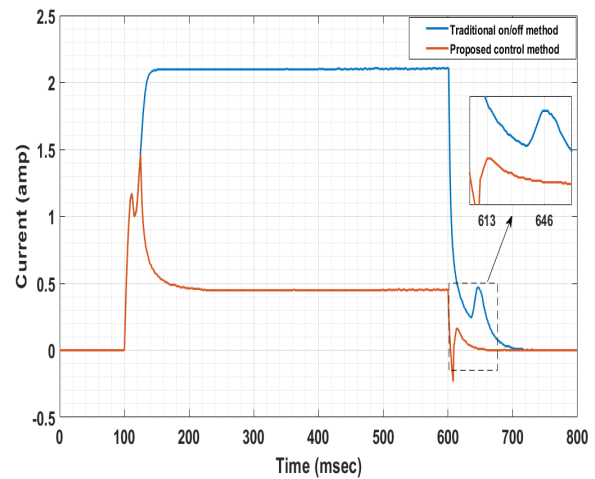


Figure 134. Solenoid current when the solenoid is energized by the traditional on/off method and the proposed control method.

The figure shows that at the beginning of solenoid energizing, the behavior of the current curves is the same. Consequently, applying the proposed control method makes the valve spool rapidly open without any oscillation. No extra time is needed for the valve spool to reach its maximum stroke position.

It is also shown that the solenoid current is reduced to holding the current value after the valve has reached its maximum stroke. The reduction of current occurs exponentially without any change in the existing slope. Accordingly, the valve spool is stationary at its maximum stroke position and does not move.

The zoomed portion of the figure shows the points at which the valve has been closed. It is shown that when the proposed method is applied, the valve spool takes only 13 msec to reach its initial position. When the traditional on/off method is used, the valve spool takes 46 msec to get its initial position and close it. So, the proposed control method reduces the valve closing time by about 72% of the traditional way.

The temperature effect is studied by measuring the valve temperature after energizing it by both the traditional on/off method and the proposed control method. PT2100 Pacer digital thermometer is used to measure the valve temperature, and the results are shown in figure 15.

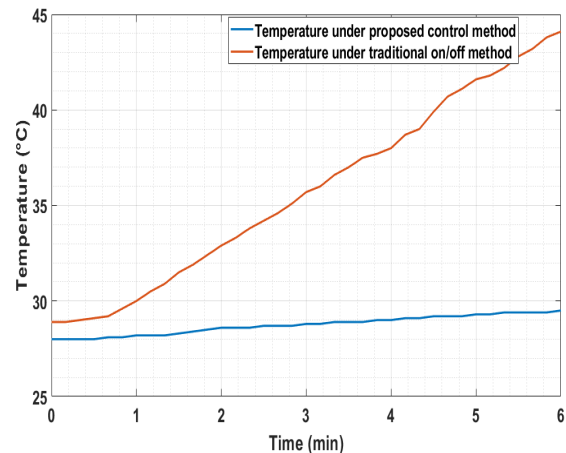


Figure 145. Temperature effect when using the traditional on/off method and the proposed control method.

The figure shows a slight increase in the valve temperature observed when using the proposed control method to energize the solenoid valve. Otherwise, a significant rise in valve temperature is observed when the valve is energized by the traditional on/off way. The temperature is shown to increase rapidly with increasing the energizing time. The increased temperature is considered a waste of energy, but it also harms the solenoid valve.

Increasing the valve temperature harms the magnetization characteristics of the solenoid. Hence, the dynamic response of the valve is affected as well. If the temperature exceeds the solenoid coil insulation layers' tolerance, these layers may melt, causing the coil resistance to increase [31]. Consequently, more current is consumed, and hence more energy is wasted.

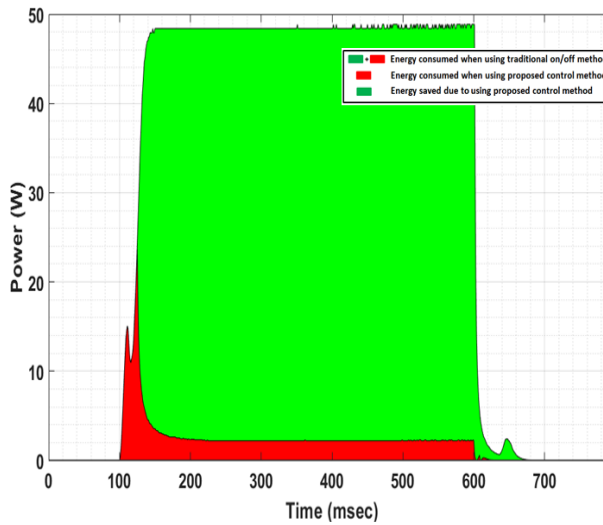


Figure 156. Power consumed energy and saved energy of the solenoid valve when it is energized by the traditional on/off method and the proposed control method.

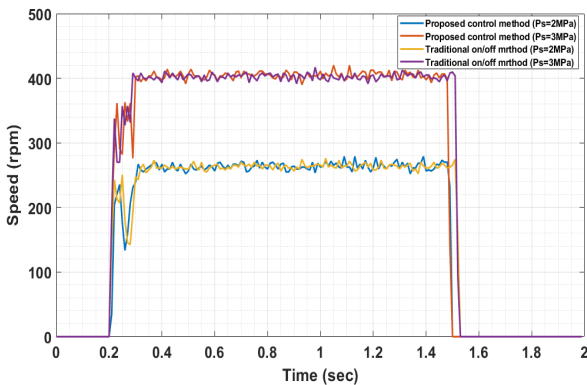


Figure 167. Hydraulic motor speed when the solenoid valve is excited by the proposed control and traditional methods under different supply pressures (2 MPa and 3 MPa).

According to the equations represented in section 3, the consumed power of the solenoid valve is calculated. Power is calculated when the valve is energized for 0.5 sec using the traditional on/off and the proposed control method. In the time-power diagram, energy is presented by the area under the curve. Consequently, power and energy results are shown in figure 16.

The saved energy depends on the solenoid valve energizing time. But, generally, the results show that

the proposed control method saves about 94% of the consumed energy when using the traditional on/off control method.

Figure 17 shows the hydraulic motor speed resulting under different supply pressure (2 MPa and 3 MPa).

The results show that, under the same supply pressure, the hydraulic motor reaches at the same time approximately the same speed. Consequently, the valve pressure and flow rate do not change when the valve is energized either by the proposed control method or by the traditional on/off. It is also shown that although the solenoid valve has been de-energized simultaneously, the hydraulic motor stops when using the proposed control method faster than when using the traditional on/off method. The proposed control method's valve closing time is shorter than the conventional on/off control method's valve closing time.

7. CONCLUSION

A new method of controlling HSVs is presented. The proposed control method is used to enhance the dynamic and energy performance of the HSVs. The proposed method uses NI myRIO as a controller while the MD10C card is used as a driver. The controller is programmed using LabVIEW software.

Validation of the proposed control method is performed under different operating conditions. Experimentally, the results show that this control method can enhance the valve performance by reducing the valve closing time, rising temperature, and consuming energy. The results show that the proposed control method can reduce the valve closing time by 72 % compared to the traditional on/off control method. The temperature rise of the valve is reduced by approximately 34% after six minutes of solenoid energizing. Also, the consumed energy is saved by about 94%.

NOMENCLATURE

U_t	Solenoid driving voltage.	[V].
i	Solenoid coil passing current.	[A].
R	Solenoid coil resistance.	[Ω].
L	Solenoid coil inductance.	[H].
μ_o	Air gap permeability	[H/m].
n	Number of solenoid coil turns.	
g_{max}	Maximum length of the air gap.	[m].
x	Valve spool position.	[m].
A	Air gap cross section area.	[m ²].
F_{mag}	Electromagnetic force.	[N].
F_{hyd}	Hydraulic force.	[N].
K	The return spring stiffness.	[N/m].
x_{pre}	The pre-loaded spring distance.	[m].
c	Damping coefficient.	[N.s/m].
m	Mass of the moving parts.	[kg].
ω	Width of the solenoid valve port.	[m].
ΔP	Pressure difference between both sides of the valve spool.	[Pa].
P_{los}	The power lost.	[W].

W_{los} The energy lost. [J].
 t Valve operating time. [s].

ACRONYMS

High-speed on/off solenoid valve.....
 (HSV).
 Pulse width modulation.....
 (PWM).
 Moving magnet actuated.....
 (MMA).

REFERENCES

- [1] H. Qiu and Q. Su, "Simulation Research of Hydraulic Stepper Drive Technology Based on High Speed On/Off Valves and Miniature Plunger Cylinders," *Micromachines*, vol. 12, p. 438, 2021.
- [2] Q. Gao, Y. Zhu, Z. Luo, N. Bruno, "Investigation on adaptive pulse width modulation control for high speed on/off valve," *Journal of Mechanical Science & Technology*, vol. 34, 2020.
- [3] N. N. Gavrilović, B. P. Rašuo, G. S. Dulikravich, V. B. Parezanović, "Commercial aircraft performance improvement using winglets," *FME Transactions*, vol. 43, pp. 1-8, 2015.
- [4] S. Wang, Z. Weng, and B. Jin, "A Performance Improvement Strategy for Solenoid Electromagnetic Actuator in Servo Proportional Valve," *Applied Sciences*, vol. 10, p. 4352, 2020.
- [5] B. P. Rašuo and A. Č. Begin, "Optimization of wind farm layout," *FME transactions*, vol. 38, pp. 107-114, 2010.
- [6] H. Kogler, "High dynamic digital control for a hydraulic cylinder drive," *Proceedings of the Institution of Mechanical Engineers, Part I: Journal of Systems and Control Engineering*, p. 09596518211028089, 2021.
- [7] H. Shi, Z. Liu, H. Wang, and X. Mei, "Design and performance analysis of hydraulic switching valve driven by magnetic shape memory alloy," *Advances in Mechanical Engineering*, vol. 13, p. 16878140211016985, 2021.
- [8] A. C. Mahato, S. K. Ghoshal, "Energy-saving strategies on power hydraulic system: An overview," *Proceedings of the Institution of Mechanical Engineers, Part I: Journal of Systems and Control Engineering*, vol. 235, pp. 147-169, 2021.
- [9] H. Nazemian, M. Masih-Tehrani, "Development of an optimized game controller for energy saving in a novel interconnected air suspension system," *Proceedings of the Institution of Mechanical Engineers, Part D: Journal of Automobile Engineering*, vol. 234, pp. 3068-3080, 2020.
- [10] M. Paloniitty, M. Linjama, "High-linear digital hydraulic valve control by an equal coded valve system and novel switching schemes,"

Proceedings of the Institution of Mechanical Engineers, Part I: Journal of Systems and Control Engineering, vol. 232, pp. 258-269, 2018.

- [11] Q. Zhong, X. Wang, G. Xie, H. Yang, C. Yu, E. Xu, *et al.*, "Analysis of Dynamic Characteristics and Power Losses of High Speed on/off Valve with Pre-Existing Control Algorithm," *Energies*, vol. 14, p. 4901, 2021.
- [12] C. Zhou, J. Li, G. Deng, "Control and jetting characteristics of an innovative jet valve with zoom mechanism and opening electromagnetic drive," *Ieee/Asme Transactions On Mechatronics*, vol. 21, pp. 1185-1188, 2015.
- [13] J. Zhao, M. Wang, Z. Wang, L. Grekhov, T. Qiu, X. Ma, "Different boost voltage effects on the dynamic response and energy losses of high-speed solenoid valves," *Applied Thermal Engineering*, vol. 123, pp. 1494-1503, 2017.
- [14] Q. Zhong, B. Zhang, H.-Y. Yang, J.-E. Ma, and R.-F. Fung, "Performance analysis of a high-speed on/off valve based on an intelligent pulse-width modulation control," *Advances in Mechanical Engineering*, vol. 9, p. 1687814017733247, 2017.
- [15] B. Zhang, Q. Zhong, J.-e. Ma, H.-c. Hong, H.-m. Bao, Y. Shi, *et al.*, "Self-correcting PWM control for dynamic performance preservation in high speed on/off valve," *Mechatronics*, vol. 55, pp. 141-150, 2018.
- [16] F. Gabdrāfikov, M. Abramov, S. Shamukaiev, I. Aysuvakov, D. Kharisov, U. Makhyanov, *et al.*, "Theoretical and experimental study of a hydraulically actuated diesel pump-injector unit with electronically controlled ring valve," *FME transactions*, vol. 47, pp. 576-584, 2019.
- [17] C.-w. Lee and O.-k. Kwon, "A highly accurate solenoid valve driver with current sensing circuits for brake systems," *IEICE Electronics Express*, p. 15.20171029, 2018.
- [18] P. Liu, L. Fan, W. Peng, X. Ma, and E. Song, "Design and Optimization of Novel High-Speed Electromagnetic Actuator for Electronic Fuel Injection System," SAE Technical Paper 0148-7191, 2017.
- [19] J. Ruan, R. Burton, "An electrohydraulic vibration exciter using a two-dimensional valve," *Proceedings of the Institution of Mechanical Engineers, Part I: Journal of Systems and Control Engineering*, vol. 223, pp. 135-147, 2009.
- [20] L. Du, Y. Wang, Y. Wang, Y. Wang, G. Zhang, and X. Zhang, "Application of Self-Propelled Light Electro-Hydraulic Servo Vibrator Vehicle: A Case of Chaganhua Town, Jilin Province, China," in *IOP Conference Series: Earth and Environmental Science*, 2021, p. 012139.
- [21] T. Xie, C. Wang, C. Yu, and M. Xiong, "Design of Large-Stroke and High-Resolution

- Drive System Based on Giant Magnetostrictive Material," *International Journal of Precision Engineering and Manufacturing*, vol. 22, pp. 799-811, 2021.
- [22] C. Noergaard, E. L. Madsen, J. M. Joergensen, J. H. Christensen, and M. M. Bech, "Test of a novel moving magnet actuated seat valve for digital displacement fluid power machines," *IEEE/ASME Transactions on Mechatronics*, vol. 23, pp. 2229-2239, 2018.
- [23] S. E. Koktavy et al. "Design of a crank-slider spool valve for switch-mode circuits with experimental validation," *Journal of Dynamic Systems, Measurement, and Control*, vol. 140, p. 061008, 2018.
- [24] K. J. T. Dizon, M. B. Niolo, J. B. D. Santos, and B. B. Zari, "Web-based Vital Sign Parameter Monitoring and Alert System using NI MyRIO."
- [25] H. Wang, Z. Chen, Y. Guo, J. Zhang, and Q. Wang, "A Queue Driven State Machine Based LabVIEW Pattern Used in Large-Scale Measuring and Controlling Systems," in *Proceedings of 2021 Chinese Intelligent Systems Conference*, 2022, pp. 795-802.
- [26] L. HUDSON INDUSTRY CO., "Solenoid operated directional control valve" https://www.hudsonindustry.com/?attachment_id=2907#main/trackback/ vol. WE10,NG10 Series structure, May 31,2015.
- [27] K. A. Ghamry, A. Saleh, and M. H. Mabrouk, "Sensorless Position Estimating and Transition time Identifying for the spool of a High Speed on/off Solenoid Valve." *FME Transactions*, Vol. 50, No, 1, pp. 99-108, 2022.
- [28] M. G. Rabie, "Fluid power engineering/M. Galal Rabie," ed: New York: McGraw-Hill, 2009.
- [29] L. Jin, Q. Wang, "Positioning control of hydraulic cylinder with unknown friction using on/off directional control valve," *Proceedings of the Institution of Mechanical Engineers, Part I: Journal of Systems and Control Engineering*, vol. 232, pp. 983-993, 2018.
- [30] M. Jin, M. Min, X. Lin, and H. Liu, "Study on control scheme of on-line measurement system for key dimension of spinning head," in *IOP Conference Series: Earth and Environmental Science*, 2020, p. 012216.
- [31] J. Zhao, P. Yue, L. Grekhov, K. Wei, and X. Ma, "Temperature and frequency dependence of electrical iron effects on electromagnetic characteristics of high-speed solenoid valve for common rail injector," *International Journal of Applied Electromagnetics and Mechanics*, vol. 60, pp. 173-185, 2019.

УШТЕДА ЕНЕРГИЈЕ И ПОБОЉШАЊЕ ПЕРФОРМАНСИ ЕЛЕКТРОМАГНЕТНОГ ВЕНТИЛА ВЕЛИКЕ БРЗИНЕ ЗА УКЉУЧИВАЊЕ/ИСКЉУЧИВАЊЕ

А.Н. Абороба, К.А. Гамри, А. Салех, М.Х. Мабрук

Електромагнетни вентили велике брзине за укључивање/искључивање (ХСВ) су дигиталне вредности које се обично користе у хидрауличним енергетским системима. Ови вентили се обично користе у контроли притиска и протока што захтева високе динамичке и енергетске перформансе да би се побољшала тачност контроле. Овај рад има за циљ да предложи нову методу контроле која се користи за побољшање динамичких и енергетских перформанси ХСВ-а.

Предложени метод је заснован на техници модулације ширине импулса (ПВМ) коју имплементирају ЛабВИЕВ софтвер и НИ миРИО. На основу тога, НИ миРИО има модул у реалном времену; није потребна повратна информација. Уведен је математички модел ХСВ-а, који описује сваки подсистем вале и његове међусобне интеракције. Предложена метода је валидирана у различитим условима рада. Резултати показују да ће примена предложене методе управљања на ХСВ смањити време затварања калема вентила за 72% и смањити потрошњу енергије за 94% у поређењу са традиционалном методом управљања укључивање/искључивање.